

Holger Bolze^{1,2,*}
Juliane Riewe^{3,5}
Heike Bunjes^{3,5}
Andreas Dietzel^{4,5}
Thomas P. Burg^{1,2,*}


Protective Filtration for Microfluidic Nanoparticle Precipitation for Pharmaceutical Applications

Microfluidic processes are of great interest for the production of nanoparticles with reproducible properties. However, in real systems, it is difficult to completely exclude incidental production of larger particles, which can contaminate the product or clog downstream process modules. A class of microfluidic filters was devised for eliminating particulate contamination in multistage continuous-flow processes. To achieve high throughput and filtration efficiency, a high-surface-area filter with an application-adapted bonding method was developed. As a model application, the filtration efficiency was analyzed for lipid nanoparticles made by microfluidic antisolvent precipitation and the results were compared with requirements of the European and US guidelines.

Keywords: In-line filtration, Lipid nanoparticles, Membrane filtration, Nanoparticle synthesis, Precipitation

Received: October 13, 2020; *revised:* December 23, 2020; *accepted:* December 23, 2020

DOI: 10.1002/ceat.202000475

 This is an open access article under the terms of the Creative Commons Attribution License, which permits use, distribution and reproduction in any medium, provided the original work is properly cited.

1 Introduction

Microfluidic processes provide outstanding control for liquid-phase syntheses due to the predictability of the laminar flow and rapid dissipation of concentration gradients by diffusion. In addition to improved precision and reproducibility, microfluidic devices enable a reduction in waste [1] and give access to high-resolution reaction time control [2]. These qualities are especially desirable in nanomaterial synthesis for pharmaceutical formulations. For example, nanocarriers improving the solubility of poorly water-soluble compounds need to fall reliably in specific size ranges for safety and effectiveness. This also applies to nanoparticle encapsulation for improving cellular uptake, controlling the drug release characteristic or for targeting specific cell types. In the last decades, several studies described the encapsulation of drugs in polymer nanoparticles [3], solid lipid nanoparticles [4, 5], and liposomes [6]. These are but a few examples representing a much wider range of materials unified by having an average particle size usually much below 500 nm. Particles in the size range of about 100 nm and below are particularly interesting with regard to tumor site targeting [3].

Many successful devices for synthesizing nanoparticles by microfluidic methods have been invented. However, comparatively little research has been devoted to the important question of downstream processing in line with these devices.

Work on microfluidic mixing has contributed significantly to enabling the synthesis of nanoparticles with defined properties by antisolvent precipitation. Devices which rely on staggered herringbone mixers [7–10], flow focusing [11–14], multilamination [15], impinging jets [16–19], single droplet formation

[20], Taylor flows [21, 22], or splitting the streams and recombining them to minimize the diffusion length [23, 24] have been described. Some groups added additional external power to intensify the mixing process, e.g., by using small rotors [25] or ultrasound [26–28].

These and other microsystems allow the generation of nanoparticles with narrow size distributions and other desirable properties for drug delivery. However, there is no guarantee that the products are completely free of microparticles. Micron-sized particles can clog blood vessels when injected, so

¹Holger Bolze, Prof. Thomas P. Burg, Ph.D.
holger.bolze@mpibpc.mpg.de

Max Planck Institute for Biophysical Chemistry, Research Group Biological Micro- and Nanotechnology, Am Fassberg 11, 37077 Göttingen, Germany.

²Holger Bolze, Prof. Thomas P. Burg, Ph.D.
thomas.burg@tu-darmstadt.de

Technische Universität Darmstadt, Department of Electrical Engineering and Information Technology, Merckstr. 25, 64283 Darmstadt, Germany.

³Juliane Riewe, Prof. Dr. Heike Bunjes

Technische Universität Braunschweig, Institut für Pharmazeutische Technologie und Biopharmazie, Mendelssohnstr. 1, 38106 Braunschweig, Germany.

⁴Prof. Dr. Andreas Dietzel

Technische Universität Braunschweig, Institute of Microtechnology, Alte Salzdahlumer Str. 203, 38124 Braunschweig, Germany.

⁵Juliane Riewe, Prof. Dr. Heike Bunjes, Prof. Dr. Andreas Dietzel

Technische Universität Braunschweig, PVZ – Center of Pharmaceutical Engineering, Franz-Liszt-Str. 35a, 38106 Braunschweig, Germany.

the level has to be limited reliably on a very low level in preparations for injection or infusion [29, 30].

In addition to microparticles expected purely on statistical grounds, microparticles may form incidentally in microfluidic systems due to a range of complex phenomena. For example, if the flow is perturbed even temporarily, larger particles can be generated. Another source of microparticle contamination can be fouling layers that are prone to deposit upon contact between an oversaturated solution and the system walls [31]. Such layers can perturb the process and even clog the microsystem. Importantly, when parts of the deposited layers are washed off, microparticles can be released in the product stream.

To face these issues, different strategies have been applied in microsystems like the conditioning of the stream [23, 32], conditioning of the channel surface [22, 23, 33], encasing with sheath streams [14, 34], or sonication [35–38].

In some studies, micromixers have been connected to microfluidic filters to remove bubbles from the product [39], impurities from the inlet [40] or to recycle unused lipid and drug [41]. Systems for the removal or fractionation of particles by inertial drift [42, 43], field-flow fractionation [44], and sound waves [45–47] have also been proposed. However, these principles are prone to disruptions by even small changes in the flow. To our knowledge, removing microparticles reliably and continuously from a microfluidic product stream, such that the requirements for parenteral drugs are satisfied, is still an open challenge.

In this study, a concept is described where the micron-sized particles are rejected by submicrometer pores of uniform size integrated in a microfluidic tangential flow filter. Although it is possible to construct such filters by in-plane features, such as pillars or slits, the required lithographic precision and the low throughput of such structures are prohibitive [40]. Therefore, a vertical design was implemented based on nanoporous filter membranes [48–52]. To fabricate the device, an improved process for bonding polycarbonate (PC) filter membranes to poly(dimethylsiloxane) (PDMS) was developed. Additionally, the degradation of the PC filter due to different cleaning procedures was characterized.

Finally, to demonstrate the applicability of the filter for a nanoparticle producing process, the device was combined with a microfluidic antisolvent precipitation system capable of producing more than 15 mL of a lipid nanoparticle dispersion in 4 h without disruption. Here, a multilamination mixer was used, but the filter could be combined with other mixing concepts like plug-flow devices [53] as well. In this study, trimyristin served as carrier lipid. Nanoparticles based on trimyristin and related triglycerides have been investigated as carriers for a variety of drugs, mostly of low molecular weight

but also including peptides, proteins, and nucleic acids [4, 5, 54–63]. The carrier particles were loaded with the dye Nile red [64] to increase the microscopic visibility for purity controls.

2 Materials and Methods

2.1 Filter Chip

The inlet channel of the filter chip fanned out into 32 smaller channels with a cross section of $100 \times 50 \mu\text{m}$ to reduce the pressure drop (Fig. 1). Each of these channels contained a 100 mm long serpentine path, which resulted in a usable filter area of 320 mm^2 . The filtrate side of the filter consisted of a chamber supported by bars to prevent a collapse of the chamber. The channel structure was made of PDMS by standard soft lithography using an SU-8 master [65]. The PDMS (Sylgard 184, Dow Chemical Company, Midland, MI) was prepared by mixing the prepolymer and the curing agent (20:1) and pouring it onto the master to a final thickness of 5 mm. The PDMS was degassed and then cured at 80°C for 1 h. The cured PDMS was removed from the SU-8 negative and cut into individual chips. Finally, fluidic inlets with a diameter slightly smaller than the used tubing were punched manually. The PDMS slabs were then cleaned with isopropanol in an ultrasonic bath.

The commercially available filter membrane had a nominal pore diameter of 400 nm (Nuclepore hydrophilic polycarbonate membrane, GE Healthcare, Chicago, IL). The membrane was machine-cut with a CO_2 laser (VLS4.60, Universal Laser Systems, Scottsdale, AZ) in a rectangular shape bigger than the chip. The filter was cleaned in isopropanol for 2 h, then dried and activated in a low-pressure oxygen plasma for 1 min at 50 W and 0.4 bar (Diener Femto, Diener Electronics, Ebhausen, Germany). The activated membrane was submerged in a 1 mass % solution of hexamethylenediamine (Merck, Darm-

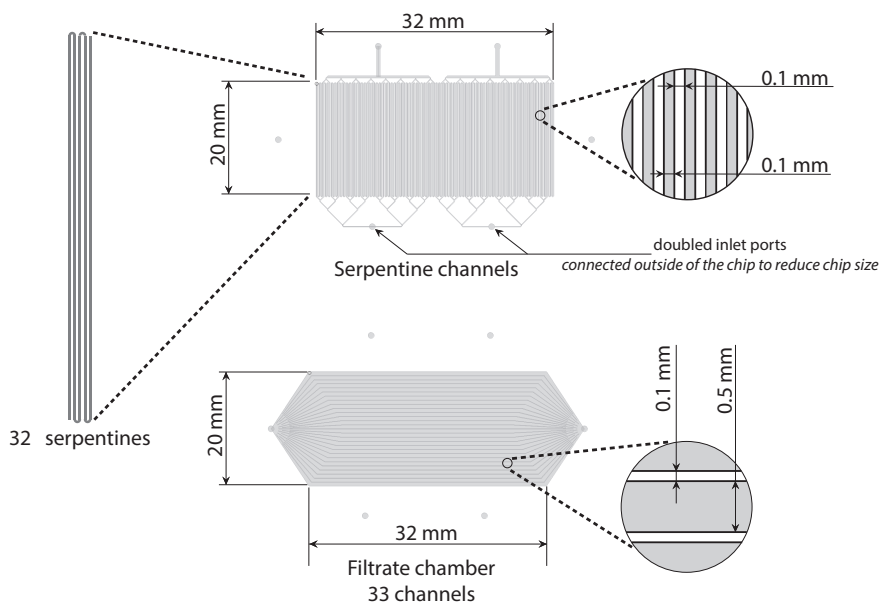


Figure 1. Structure of the used filter chip.

stadt, Germany) under argon atmosphere for 24 h. Then the membrane was rinsed with water and dried before activating it again in an oxygen plasma and silanizing it with (3-aminopropyl)trimethoxysilane (Merck, Darmstadt, Germany) in vacuum at 80 °C to enable a bonding between membrane and PDMS.

For bonding, the silanized membrane and the PDMS parts were activated in an oxygen plasma and pressed together to form elemental bonds between the components. At first, the membrane was placed on the serpentine and pressed carefully on the PDMS to prevent wrinkles between the elements, then the chamber was aligned according to the serpentine layer on the membrane. To accelerate the bonding process, the chip was heated for 1 h to 80 °C. Small pieces of capillary tubing (FEP tubing, Trajan Scientific and Medical, Melbourne, Australia) were inserted into the punched holes and sealed with epoxy (Loctite Double Bubble, Henkel, Düsseldorf, Germany). The sides of the chip were sealed by PDMS to prevent small leakages.

The filter chip assembly was placed in a custom-made holder for easy access to both sides of the device, while at the same time stabilizing the tubing against bending. A small vial was connected by a low dead volume connector to a capillary tube inserted into a vial. The vial was pressurized by a pressure controller allowing up to 1 bar overpressure of nitrogen on the vial. The other chip accesses to the serpentine side were closed with fluidic stoppers, while the filtrate accesses were connected to vials with syringe needles to prevent a pressure buildup.

2.2 Precipitation Setup

To demonstrate the applicability of the filter, lipid nanoparticles were precipitated in a multilamination mixer already described before [66]. A solvent-antisolvent process precipitated the particles. So, the lipid, stabilizer, and drug were dissolved in an organic solvent and mixed with an excess amount of water. This mixture was dominated by water, reducing the solubility of lipid and drug to a negligible amount. The supersaturated components started to precipitate and formed nanoparticles when the components were well mixed. To reach a high goodness of mixture, the mixer split the reactants in 20 separate streams and recombined them in a laminated stream in a single rectangular $30 \times 50 \mu\text{m}$ microchannel. To reduce fouling, the system was sonicated permanently at a frequency of 500 kHz. The process was already validated as a stable method to generate nanoparticles and used as a fixed system to generate nanoparticles.

The steady process typically generated particles with a mean diameter of $80 \pm 2 \text{ nm}$ and a polydispersity (i.e., width of the peak divided by the height) of $34 \pm 4 \%$ as measured by dynamic light scattering (DynaPro NanoStar, Wyatt Technology, Santa Barbara, CA). This size varied between the batches by roughly 10 nm, but for this study the exact size of the nanoparticles was of limited importance. According to the size and the used amount of lipid, a nanoparticle concentration of 1×10^{11} particles per milliliter was expected. The relatively stable concentration of microparticles was measured by vacuum filtration described in Sect. 2.4. Typically, the product contained 4.5×10^4 microparticles per milliliter with a mean diameter of $9 \mu\text{m}$ dis-

tributed in a typical Gaussian curve with the exception of a few much bigger particles (Fig. 2). More importantly, in relation to pharmacopeial guidelines, the dispersion contained around 42.5 particles per milliliter bigger than $12 \mu\text{m}$ and 2.5 particles per milliliter even bigger than $25 \mu\text{m}$. The system itself ran stable for about 4 h on average before the mixing chip clogged or the experiment was stopped.

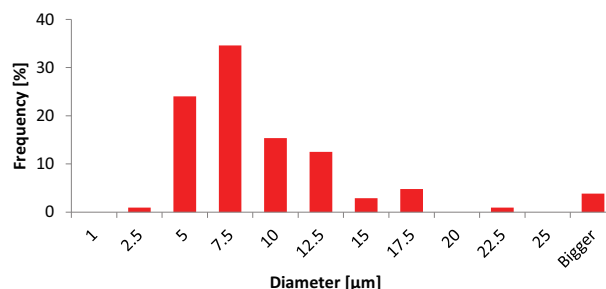


Figure 2. Histogram of microparticles detected on the filter.

2.3 Solutions

The organic solution used for stable particle precipitation consisted of 0.79 mg mL^{-1} trimyristin, 5 mg mL^{-1} polysorbate 80, and $8 \mu\text{g mL}^{-1}$ Nile red in acetone. All chemicals were from Merck, Darmstadt, Germany. Purified water served as antisolvent. All solutions were filtered by a 200-nm syringe filter (polypropylene; VWR International, Radnor, PA) to prevent clogging. The membrane filter was characterized by a suspension of fluorescent latex nanoparticles in water. The suspension contained 5.68×10^4 particles per milliliter of $20 \mu\text{m}$ big particles and 4.55×10^5 particles per milliliter of $10 \mu\text{m}$ big particles (size in diameter; Fluoresbrite YG, Polysciences, Warrington, PA).

2.4 Analytics

The content of microparticles was analyzed by vacuum filtration. This detection method used a filter membrane to collect particles on the surface of the membrane, which was analyzed by a microscope (Axioscope D1m with Filterset 75 HE and 44, Zeiss, Oberkochen, Germany, and a CCD camera Andor Clara, Andor Technologies, Belfast, Great Britain). The used surface of the membrane was limited to 0.22 cm^2 by glass components to intensify the amount of sample applied per area. The membrane used for analysis was the same as implemented in the microfluidic filter. To suck the sample, usually between 1 and 3 mL, through the membrane, a vacuum was applied in the Erlenmeyer flask used to collect the filtrate.

After filtrating the sample, the device was rinsed with 15 mL water containing polysorbate 80 in the same concentration as in the dispersion, to move microparticles from the glass components on the filter and nanoparticles through it. The membrane was dried and transferred from the filtration apparatus to the microscope. Due to the size of the microparticles, the

microscope could be used to measure their size. This allowed the determination of the mean size and the fractions that breached the pharmaceutical thresholds. Since the volume of the sample was defined, the concentration of these fractions could be calculated. To ease the detection, the particles were labeled by the fluorescent dye Nile Red. The content of trimyristine was measured by high-performance liquid chromatography.

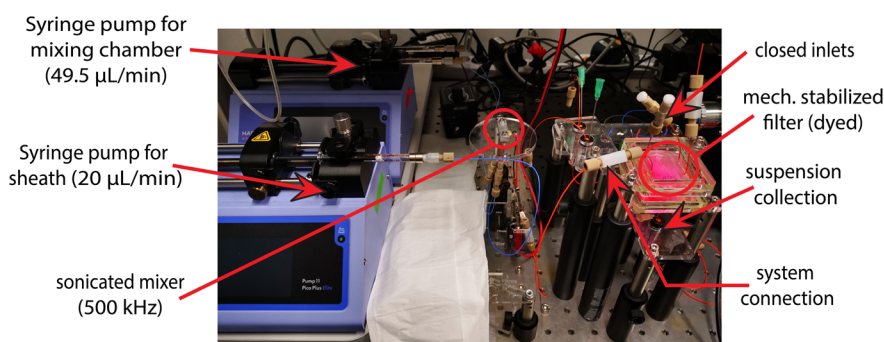


Figure 3. Combination of precipitation and filtration setup into a single system.

2.5 Microfluidic Filtration Experiments

The performance of the microfluidic filters was analyzed using suspensions containing the reference particles. The suspension was filled in the vial and pressurized at 0.2 bar overpressure. Every 2 h the chip was cleaned by flowing Hellmanex III (Helma, Müllheim, Germany) through the other end of the serpentine and the filtrate side to remove particle aggregates on the filter. After purging, the filtrate collected during the following 10 min of the experiment were discarded to remove residues of the purging solution. After the experiment, 3 mL of the filtrate was analyzed by vacuum filtration.

In experiments in which the filter was connected directly downstream of the microfluidic nanoparticle synthesis, capillary tubing and low-volume connectors (NanoTight Unions, IDEX Health & Science, Lake Forest, IL) were employed to connect the two devices (Fig. 3). The solvent was injected at a rate of $4.5 \mu\text{L min}^{-1}$, while the antisolvent was injected at $45 \mu\text{L min}^{-1}$. The sheath fluid (water) was injected at $20 \mu\text{L min}^{-1}$.

3 Results and Discussion

3.1 Needed Filtration Efficiency

According to the US Pharmacopeia and European Pharmacopeia [29, 30], a parenteral suspension is limited to 12 particles with a diameter of more than $10 \mu\text{m}$ (cat I) per milliliter and only 2 particles with a diameter of more than $25 \mu\text{m}$ (cat II) per milliliter.

According to the analysis of the precipitated dispersion, the product contained 42.5 cat I and 2.5 cat II particles per milliliter. The exceeding of the limits meant that the product has to be filtered. This issue was increased by the low concentration of lipid in the product. While the product of the system used in this study contained only 0.012 % of lipid by mass, common formulations based on lipid nanoparticles typically contain 10 mass % of lipid phase [63]. This difference meant that for a pharmaceutical application the product would have to be concentrated up to 826 times, which was rounded up to a 1000 times to take into account process irregularities. A concentration by a factor of 1000 would increase the concentration of micron-sized particles correspondingly, leading to an effective product concentration of 42 500 cat I and 2500 cat II par-

ticles per milliliter. To satisfy the above-mentioned pharmacopoeial requirements for a 1000 times concentrated version of the precipitated dispersion, the filter would have to reach a filtration efficiency of 99.97 % for cat I and 99.91 % for cat II particles.

The vacuum filtration used for particle detection has a lower detection limit due to the limited volume that can be sampled. Considering the sample size, the microscopy technique, and a security margin to prevent influences from random fluctuations, the detection limit was estimated to 37 particles per milliliter. This threshold combined with the low concentration of cat I and II in the product and the high target purity meant that more than 500 mL of produced dispersion would be needed to control the quality of the filtrate with adequate statistics. To produce such a volume for a single test would require ten weeks with the microfluidic device. Therefore, fluorescent reference particles were used in the experiments, which had a much higher concentration than the precipitated microparticles.

3.2 Efficiency of the Filter

Although filters are typically classified by their nominal pore size, real filters show a distribution of pore sizes related to the mechanism of pore generation. In this study, track-etched filter membranes known for their narrow pore size distribution compared to other types were employed. But even these filters had some larger pores, since the pores were positioned randomly and overlap between two or more pores was common (Fig. 4). To obtain a best case estimate of the real efficiency of the filter membrane, vacuum filtration was employed to characterize membranes that were not yet integrated into the microfluidic system. To compare the membranes and microfluidic filter, the filtration efficiency was measured, which was calculated by Eq. (1).

$$\begin{aligned} \text{Efficiency}[\%] &= \left(1 - \frac{\text{Particles per milliliter in filtered solution}}{\text{Particles per milliliter in unfiltered solution}} \right) \cdot 100 \end{aligned} \quad (1)$$

The experiments indicated that the material was capable to retain up to 100 % in both categories of the reference microparticles. In a few experiments, some particles with a size of $20 \mu\text{m}$

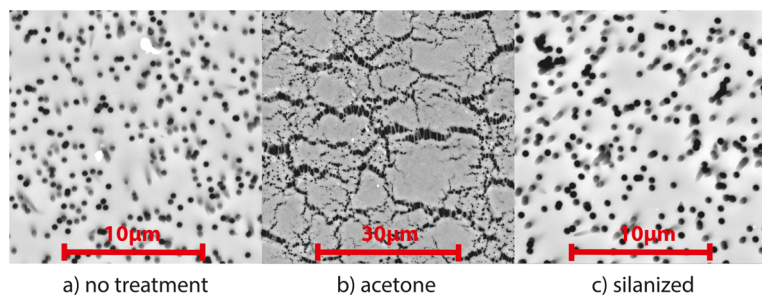


Figure 4. Electron micrographs of a track etched membrane illustrating the damaging of the material by an organic solvent and the intact surface after the silanization process.

could pass the filter, lowering the efficiency to 99.6%, which would disqualify the filter from use in a real application scenario and hint at an already damaged membrane, maybe by the mechanical handling of the membrane by tweezers and the vacuum filtration device. This meant, while some membranes reached the quality needed, a few showed too low efficiency even without the microfluidic integration process.

There was a concern that solvent cleaning and ultrasonication done during the microfluidic integration process would degrade the membrane [67]. The membrane consisted of polycarbonate, which was susceptible to interaction with organic solvents leading to a destruction of the pore structure (Fig. 4). Since such destruction could harm the filtration efficiency without destroying the membrane in total, the efficiency of the silanized filter material was tested without bonding to the chip to ensure that the silanization does not harm the membrane. The experiments provided the same high efficiencies as untreated membranes, so the process itself left the membrane intact.

In the next step, the filtration efficiency of completely assembled microfluidic devices was analyzed (Fig. 5). Out of ten microfluidic filtration devices tested, three were judged acceptable, as their attained filtration efficiency exceeded the target requirement. Another four almost satisfied the requirement, while three devices had efficiencies below 90% to a worst case of 56%.

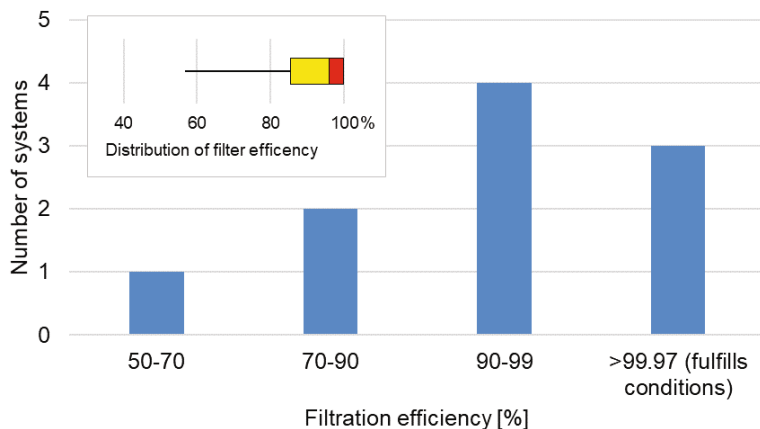


Figure 5. Filtration efficiency of systems from one production batch which contained ten systems that passed the basic functionality test (open ports, no leakages). The diagram shows the more often undercut cat I criteria and 10- μ m particles.

These results suggested that the filtration performance of at least some of the devices was degraded by the microfluidic integration process. This conclusion was supported by the vacuum filtration results above, which showed that membranes that were cleaned and silanized but not integrated in the PDMS device, showed superior filtration efficiency. A possible explanation could be the mechanical handling and alignment of the membrane or mechanical stress induced by the heating of the assembled materials due to the different thermal expansion coefficients of PDMS and polycarbonate.

However, the results also showed that very high efficiencies were achieved with a significant fraction of the devices. Thus, higher yield is expected if rigorous quality control is applied to take only devices with acceptable filtration efficiency and if the assembly process is optimized to minimize mechanical stress on the membrane. The filters fulfilling the cat I and cat II conditions were tested repeatedly, which lead to similar results as in first experiments with minor variations of 0.016% of filter efficiency on average.

The size distributions of particles before and after the microfluidic filter were detected by vacuum filtration and microscopy. Results of these analyses are reported here only for the group of filters exhibiting less than 99.97% filtration efficiency, which is needed to fulfill the above described criterion for 10- μ m particles, since the filters with an efficiency of >99% let pass too few particles to analyze even after combining all successful experiments.

Filters with efficiencies between 70 and 99% (Fig. 6) on average yielded a reduction of the 20- μ m fraction and a small shift of the average size of the 10- μ m fraction from 11 to 9 μ m. These changes showed that filter defects allowed particles of all sizes to pass, but the smaller particles were slightly preferred.

In comparison to this result, systems with a filtration efficiency below 70% did not pass any detectable number of 20- μ m particles (Fig. 6), while the distribution of 10- μ m particles was unaltered. These results could be explained by defects with an effective size in the 10–20 μ m range, through which 10- μ m particles could pass while bigger particles were retained.

The amount of liquid pressed through the filter was limited by the stability of the membrane and the bond between PDMS and polycarbonate. Transmembrane pressures of 0.2 bar allowed stable operation of the filter and were used in most experiments. However, pressures of 0.8 bar often lead to leakage of the PDMS/polycarbonate bond. In some cases, the pressure ruptured the membrane itself and led to internal leakages. This result indicated that the bond is still a weak point of the system and should be further improved.

In an ideal filter, the throughput through the membrane should not influence the filtration efficiency, since the restricting mechanism by pores is independent of the flow rate. The real filters on the other side are burdened by defects in the form of leakages or thinned material. Such defects can react on increased pressure by a higher throughput of

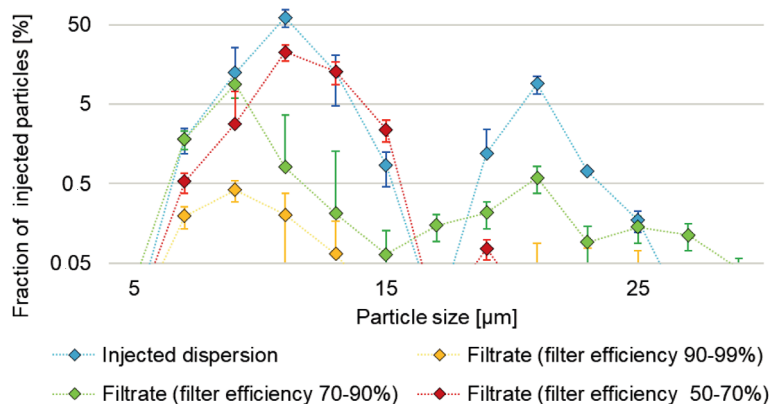


Figure 6. Size distributions of different filtrates and the injected dispersion.

liquid and microparticles or even can be widened to major ruptures.

3.3 Combination of Systems

The first result of the serial integration of the particle synthesis and filtration systems was that the filter was capable of processing a stream of $70 \mu\text{L min}^{-1}$ without leakage or immediate clogging. Single filter chips were used for up to three production cycles of 8 h per round without detectable quality degradation, which proved the long-term stability of the filters for long-time production processes.

The filtrate was analyzed to compare the lipid content before and after the filtration by HPLC. The analysis showed a reduction of the lipid concentration from 121 to 106 mg mL^{-1} . According to this, 87 % of the lipid passed the filter as nanoparticles. Based on the concentration and mean size of the microparticles measured in the unfiltered dispersion, the mass of lipid contained in the captured microparticles can be estimated as 0.08 mg mL^{-1} . In comparison to the mass captured in the filter, only 0.5 % of the loss could thus be related to microparticles, so another mechanism had to be active that retained more than 10 % of the produced nanoparticles. A possible candidate for this mechanism was the capturing of particles, which get into contact with the system walls, as observed for other kinds of particles [68–70].

According to this loss mechanism, the pore size should be increased to lower the loss of nanoparticles, but this would be a topic for further investigations since this study was focused on the proof-of-concept and used only a single pore size.

4 Conclusion

Continuous production of nanoparticles for parenteral application with pharmacopoeial-grade purity in microfluidic systems is a challenging task due to the strict limit for microparticle contamination. The results of this study indicate that these requirements can be met using microfluidics with integrated nanofilters.

To elucidate the potential and limitations of this class of devices, a microfluidic filter capable of handling the volume of

a real microfluidic production system for lipid nanoparticles was constructed. By defining the maximum allowed microparticle concentration based on regulations, measuring technique, and precipitated nanoparticle concentration, it could be confirmed that the newly designed filter system can process the produced dispersion to secure low microparticle levels. However, not all of the tested devices attained the same filtration efficiency as membranes that were not integrated in a microfluidic system. It is likely that mechanical stress during the fabrication process was the cause of this difference, and this will be addressed in the future by more systematic studies and process optimization.

Yet, another interesting development will be to exploit the tangential-flow capability of the device to remove the filter cake. By recirculating the nanoparticle dispersion entering the filter out of and back into an open reservoir, the filter could operate continuously and independent of the flow rate imposed by the microfluidic synthesis. This is expected to increase the operation time and reduce the number of nanoparticles held back by the filter cake.

Ultimately, one can envision that the combination of synthesis and downstream purification will help to lower the production cost and increase the quality of nanoparticle systems for applications in drug delivery.

Acknowledgment

Holger Bolze and Juliane Riewe acknowledge support by scholarships of the ‘ μ -Props – Processing of Poorly Soluble Drugs at Small Scale’ program provided by the Niedersächsisches Ministerium für Wissenschaft und Kultur (MWK) of the Federal State of Lower Saxony (Germany) and Boehringer Ingelheim, respectively. Heike Bunjes acknowledges support from the MWK of Lower Saxony (Germany) within the SMART BIOTECS alliance. Open access funding enabled and organized by Projekt DEAL.

The authors have declared no conflict of interest.

Abbreviations

cat I	particles bigger than $10 \mu\text{m}$
cat II	particles bigger than $25 \mu\text{m}$
PDMS	poly(dimethylsiloxane)

References

- [1] L. Grundemann, V. Gonschorowski, N. Fischer, S. Scholl, *J. Cleaner Prod.* **2012**, *24*, 92–101. DOI: <https://doi.org/10.1016/j.jclepro.2011.11.010>
- [2] J. Yoshida, Y. Takahashi, A. Nagaki, *Chem. Commun.* **2013**, *49* (85), 9896–9904. DOI: <https://doi.org/10.1039/c3cc44709j>
- [3] S. Acharya, S. K. Sahoo, *Adv. Drug Delivery Rev.* **2011**, *63* (3), 170–183. DOI: <https://doi.org/10.1016/j.addr.2010.10.008>

- [4] A. Gordillo-Galeano, C. E. Mora-Huertas, *Eur. J. Pharm. Biopharm.* **2018**, *133*, 285–308. DOI: <https://doi.org/10.1016/j.ejpb.2018.10.017>
- [5] W. Mehnert, K. Mäder, *Adv. Drug Delivery Rev.* **2012**, *64*, 83–101. DOI: <https://doi.org/10.1016/j.addr.2012.09.021>
- [6] T. M. Allen, P. R. Cullis, *Adv. Drug Delivery Rev.* **2013**, *65* (1), 36–48. DOI: <https://doi.org/10.1016/j.addr.2012.09.037>
- [7] M. Maeki, T. Saito, Y. Sato, T. Yasui, N. Kaji, A. Ishida, H. Tani, Y. Baba, H. Harashima, M. Tokeshi, *RSC Adv.* **2015**, *5* (57), 46181–46185. DOI: <https://doi.org/10.1039/c5ra04690d>
- [8] I. V. Zhigaltsev, N. Belliveau, I. Hafez, A. K. K. Leung, J. Huft, C. Hansen, P. R. Cullis, *Langmuir* **2012**, *28* (7), 3633–3640. DOI: <https://doi.org/10.1021/la204833h>
- [9] N. M. Belliveau, J. Huft, P. J. C. Lin, S. Chen, A. K. K. Leung, T. J. Leaver, A. W. Wild, J. B. Lee, R. J. Taylor, Y. K. Tam, C. L. Hansen, P. R. Cullis, *Mol. Ther. Nucleic Acids* **2012**, *1*, E37. DOI: <https://doi.org/10.1038/mtna.2012.28>
- [10] Y. Morikawa, T. Tagami, A. Hoshikawa, T. Ozeki, *Biol. Pharm. Bull.* **2018**, *41* (6), 899–907. DOI: <https://doi.org/10.1248/bpb.b17-01036>
- [11] R. R. Hood, D. L. DeVoe, *Small* **2015**, *11* (43), 5790–5799. DOI: <https://doi.org/10.1002/sml.201501345>
- [12] A. Jahn, S. M. Stavis, J. S. Hong, W. N. Vreeland, D. L. Devoe, M. Gaitan, *ACS Nano* **2010**, *4* (4), 2077–2087. DOI: <https://doi.org/10.1021/nn901676x>
- [13] J. M. Lim, N. Bertrand, P. M. Valencia, M. Rhee, R. Langer, S. Jon, O. C. Farokhzad, R. Karnik, *Nanomedicine* **2014**, *10* (2), 401–409. DOI: <https://doi.org/10.1016/j.nano.2013.08.003>
- [14] M. Rhee, P. M. Valencia, M. I. Rodriguez, R. Langer, O. C. Farokhzad, R. Karnik, *Adv. Mater.* **2011**, *23* (12), H79–H83. DOI: <https://doi.org/10.1002/adma.201004333>
- [15] F. Bally, D. K. Garg, C. A. Serra, Y. Hoarau, N. Anton, C. Brochon, D. Parida, T. Vandamme, G. Hadziioannou, *Polymer* **2012**, *53* (22), 5045–5051. DOI: <https://doi.org/10.1016/j.polymer.2012.08.039>
- [16] M. Akbulut, P. Ginart, M. E. Gindy, C. Theriault, K. H. Chin, W. Soboyejo, R. K. Prud'homme, *Adv. Funct. Mater.* **2009**, *19* (5), 718–725. DOI: <https://doi.org/10.1002/adfm.200801583>
- [17] B. K. Johnson, R. K. Prud'homme, *AIChE J.* **2003**, *49* (9), 2264–2282. DOI: <https://doi.org/10.1002/aic.690490905>
- [18] H. Nagasawa, N. Aoki, K. Mae, *Chem. Eng. Technol.* **2005**, *28* (3), 324–330. DOI: <https://doi.org/10.1002/ceat.200407118>
- [19] S. Watanabe, T. Hiratsuka, Y. Asahi, A. Tanaka, K. Mae, M. T. Miyahara, *Part. Part. Syst. Charact.* **2015**, *32* (2), 234–242. DOI: <https://doi.org/10.1002/ppsc.201400126>
- [20] T. Lorenz, S. Bojko, H. Bunjes, A. Dietzel, *Lab Chip* **2018**, *18*, 627–638. DOI: <https://doi.org/10.1039/c7lc01313b>
- [21] P. Erfle, J. Riewe, H. Bunjes, A. Dietzel, *Microfluid. Nanofluid.* **2017**, *21* (12), 179. DOI: <https://doi.org/10.1007/s10404-017-2016-2>
- [22] P. Erfle, J. Riewe, H. Bunjes, A. Dietzel, *Micromachines* **2019**, *10* (4), 220. DOI: <https://doi.org/10.3390/mi10040220>
- [23] J. Wagner, J. M. Kohler, *Nano Lett.* **2005**, *5* (4), 685–691. DOI: <https://doi.org/10.1021/nl050097t>
- [24] A. Kolbl, M. Kraut, K. Schubert, *Chem. Eng. J.* **2010**, *160* (3), 865–872. DOI: <https://doi.org/10.1016/j.cej.2010.02.037>
- [25] T. Q. Chastek, K. Iida, E. J. Amis, M. J. Fasolka, K. L. Beers, *Lab Chip* **2008**, *8* (6), 950–957. DOI: <https://doi.org/10.1039/b718235j>
- [26] P. H. Huang, S. G. Zhao, H. Bachman, N. Nama, Z. S. Li, C. Y. Chen, S. J. Yang, M. X. Wu, S. P. Zhang, T. J. Huang, *Adv. Sci.* **2019**, *6* (19), 1900913. DOI: <https://doi.org/10.1002/advs.201900913>
- [27] M. R. Rasouli, M. Tabrizian, *Lab Chip* **2019**, *19* (19), 3316–3325. DOI: <https://doi.org/10.1039/c9lc00637k>
- [28] F. Castro, S. Kuhn, K. Jensen, A. Ferreira, F. Rocha, A. Vicente, J. A. Teixeira, *Chem. Eng. Sci.* **2013**, *100*, 352–359. DOI: <https://doi.org/10.1016/j.ces.2013.01.002>
- [29] *United States Pharmacopeia (USP)*, 42. ed., U. S. P. Convention, USP, Rockville, MD **2019**, Ch. 788.
- [30] *European Pharmacopoeia*, 9. ed., Council of Europe, Strasbourg **2019**, Ch. 2.9.20.
- [31] M. Schoenitz, L. Grundemann, W. Augustin, S. Scholl, *Chem. Commun.* **2015**, *51* (39), 8213–8228. DOI: <https://doi.org/10.1039/c4cc07849g>
- [32] J. L. Perry, S. G. Kandlikar, *Microfluid. Nanofluid.* **2008**, *5* (3), 357–371. DOI: <https://doi.org/10.1007/s10404-007-0254-4>
- [33] N. R. Glass, R. Tjeung, P. Chan, L. Y. Yeo, J. R. Friend, *Bio-microfluidics* **2011**, *5* (3), 036501. DOI: <https://doi.org/10.1063/1.3625605>
- [34] H. Nagasawa, K. Mae, *Ind. Eng. Chem. Res.* **2006**, *45* (7), 2179–2186. DOI: <https://doi.org/10.1021/ie050869w>
- [35] R. L. Hartman, J. R. Naber, N. Zaborenko, S. L. Buchwald, K. F. Jensen, *Org. Process Res. Dev.* **2010**, *14* (6), 1347–1357. DOI: <https://doi.org/10.1021/op100154d>
- [36] S. Kuhn, T. Noel, L. Gu, P. L. Heider, K. F. Jensen, *Lab Chip* **2011**, *11* (15), 2488–2492. DOI: <https://doi.org/10.1039/c1lc20337a>
- [37] T. Noel, J. R. Naber, R. L. Hartman, J. P. McMullen, K. F. Jensen, S. L. Buchwald, *Chem. Sci.* **2011**, *2* (2), 287–290. DOI: <https://doi.org/10.1039/c0sc00524j>
- [38] J. Sedelmeier, S. V. Ley, I. R. Baxendale, M. Baumann, *Org. Lett.* **2010**, *12* (16), 3618–3621. DOI: <https://doi.org/10.1021/ol101345z>
- [39] J. H. Tsai, L. W. Lin, *Sens. Actuators, A* **2002**, *97–8*, 665–671. DOI: [https://doi.org/10.1016/s0924-4247\(02\)00031-6](https://doi.org/10.1016/s0924-4247(02)00031-6)
- [40] M. Lee, M. J. Lopez-Martinez, A. Baraket, N. Zine, J. Esteve, J. A. Plaza, N. Ahmed, A. Elaissari, N. Jaffrezic-Renault, A. Errachid, *J. Appl. Polym. Sci.* **2015**, *132* (25), 42088. DOI: <https://doi.org/10.1002/app.42088>
- [41] N. Dimov, E. Kastner, M. Hussain, Y. Perrie, N. Szita, *Sci. Rep.* **2017**, *7*, 12045. DOI: <https://doi.org/10.1038/s41598-017-11533-1>
- [42] A. Al-Halhouli, W. Al-Faqheri, B. Alhamarneh, L. Hecht, A. Dietzel, *Micromachines* **2018**, *9* (4), 171. DOI: <https://doi.org/10.3390/mi9040171>
- [43] A. A. S. Bhagat, S. S. Kuntaegowdanahalli, I. Papautsky, *Microfluid. Nanofluid.* **2009**, *7* (2), 217–226. DOI: <https://doi.org/10.1007/s10404-008-0377-2>
- [44] P. Reschiglian, M. H. Moon, *J. Proteomics* **2008**, *71* (3), 265–276. DOI: <https://doi.org/10.1016/j.jprot.2008.06.002>
- [45] J. J. Hawkes, W. T. Coakley, *Sens. Actuators, B* **2001**, *75* (3), 213–222. DOI: [https://doi.org/10.1016/s0925-4005\(01\)00553-6](https://doi.org/10.1016/s0925-4005(01)00553-6)

- [46] A. Nilsson, F. Petersson, H. Jonsson, T. Laurell, *Lab Chip* **2004**, *4* (2), 131–135. DOI: <https://doi.org/10.1039/b313493h>
- [47] F. Petersson, L. Aberg, A. M. Sward-Nilsson, T. Laurell, *Anal. Chem.* **2007**, *79* (14), 5117–5123. DOI: <https://doi.org/10.1021/ac070444e>
- [48] B.-h. Chueh, D. Huh, C. R. Kyrtos, T. Houssin, N. Futai, S. Takayama, *Anal. Chem.* **2007**, *79* (9), 3504–3508. DOI: <https://doi.org/10.1021/ac062118p>
- [49] C. G. Sip, A. Folch, *Biomicrofluidics* **2014**, *8* (3), 036504. DOI: <https://doi.org/10.1063/1.4883075>
- [50] D. Wu, A. J. Steckl, *Lab Chip* **2009**, *9* (13), 1890–1896. DOI: <https://doi.org/10.1039/b823409d>
- [51] H. B. Wei, B. H. Chueh, H. L. Wu, E. W. Hall, C. W. Li, R. Schirhagl, J. M. Lin, R. N. Zare, *Lab Chip* **2011**, *11* (2), 238–245. DOI: <https://doi.org/10.1039/c0lc00121j>
- [52] K. Aran, A. Fok, L. A. Sasso, N. Kamdar, Y. Guan, Q. Sun, A. Uendar, J. D. Zahn, *Lab Chip* **2011**, *11* (17), 2858–2868. DOI: <https://doi.org/10.1039/c1lc20080a>
- [53] P. Erfle, J. Riewe, H. Bunjes, A. Dietzel, *Microfluid. Nanofluid.* **2017**, *21* (12), 179. DOI: <https://doi.org/10.1007/s10404-017-2016-2>
- [54] Sumera, A. Anwar, M. Ovais, A. Khan, A. Raza, *IET Nano-biotechnol.* **2017**, *11* (6), 621–629. DOI: <https://doi.org/10.1049/iet-nbt.2017.0001>
- [55] A. J. Almeida, E. Souto, *Adv. Drug Delivery Rev.* **2007**, *59* (6), 478–490. DOI: <https://doi.org/10.1016/j.addr.2007.04.007>
- [56] S. Kumar, J. K. Randhawa, *Mater. Sci. Eng., C* **2013**, *33* (4), 1842–1852. DOI: <https://doi.org/10.1016/j.msec.2013.01.037>
- [57] N. Dudhipala, K. Veerabrahma, *Drug Dev. Ind. Pharm.* **2015**, *41* (12), 1968–1977. DOI: <https://doi.org/10.3109/03639045.2015.1024685>
- [58] L. B. Jensen, E. Magnusson, L. Gunnarsson, C. Vermehren, H. M. Nielsen, K. Petersson, *Int. J. Pharm.* **2010**, *390* (1), 53–60. DOI: <https://doi.org/10.1016/j.ijpharm.2009.10.022>
- [59] M. K. Lee, S. J. Lim, C. K. Kim, *Biomaterials* **2007**, *28* (12), 2137–2146. DOI: <https://doi.org/10.1016/j.biomaterials.2007.01.014>
- [60] Y. W. Naguib, B. L. Rodriguez, X. R. Li, S. D. Hursting, R. O. Williams, Z. R. Cui, *Mol. Pharm.* **2014**, *11* (4), 1239–1249. DOI: <https://doi.org/10.1021/mp4006968>
- [61] A. P. Nayak, W. Tiyafoonchai, S. Patankar, B. Madhusudhan, E. B. Souto, *Colloids Surf., B* **2010**, *81* (1), 263–273. DOI: <https://doi.org/10.1016/j.colsurfb.2010.07.020>
- [62] E. Kupetz, H. Bunjes, *J. Controlled Release* **2014**, *189*, 54–64. DOI: <https://doi.org/10.1016/j.jconrel.2014.06.007>
- [63] K. M. Rosenblatt, H. Bunjes, *Eur. J. Pharm. Biopharm.* **2017**, *117*, 49–59. DOI: <https://doi.org/10.1016/j.ejpb.2017.03.010>
- [64] P. Greenspan, S. D. Fowler, *J. Lipid Res.* **1985**, *26* (7), 781–789.
- [65] D. C. Duffy, J. C. McDonald, O. J. A. Schueller, G. M. Whitesides, *Anal. Chem.* **1998**, *70* (23), 4974–4984. DOI: <https://doi.org/10.1021/ac980656z>
- [66] H. Bolze, J. Riewe, H. Bunjes, A. Dietzel, T. P. Burg, *Conf. Proc. of the MikroSystemTechnik Kongress 2017*, **2017**, 289–292.
- [67] D. Chen, L. K. Weavers, H. W. Walker, *Ultrason. Sonochem.* **2006**, *13* (5), 379–387. DOI: <https://doi.org/10.1016/j.ultrsonch.2005.07.004>
- [68] T. Y. Ling, J. Wang, D. Y. H. Pui, *J. Nanopart. Res.* **2011**, *13* (10), 5415–5424. DOI: <https://doi.org/10.1007/s11051-011-0529-2>
- [69] S. C. Chen, Y. R. Hu, D. Y. H. Pui, J. Wang, *J. Aerosol. Sci.* **2016**, *100*, 108–117. DOI: <https://doi.org/10.1016/j.jaerosci.2016.07.008>
- [70] B. Y. H. Liu, K. W. Lee, *Environ. Sci. Technol.* **1976**, *10* (4), 345–350. DOI: <https://doi.org/10.1021/es60115a002>